Designing 129 Xe NMR Biosensors for Matrix Metalloproteinase Detection

7 AUTHORS, INCLUDING:

Philip Aru Hill
University of Pennsylvania
12 PUBLICATIONS   **371** CITATIONS

Ivan J Dmochowski
University of Pennsylvania
80 PUBLICATIONS   **1,777** CITATIONS

Designing ^{129}Xe NMR Biosensors for Matrix Metalloproteinase Detection

Qian Wei,[†] Garry K. Seward,[†] P. Aru Hill,[†] Brian Patton,[‡] Ivan E. Dimitrov,[§] Nicholas N. Kuzma,[‡,⊥] and Ivan J. Dmochowski*,[†]

Contribution from the Department of Chemistry, University of Pennsylvania, Department of Physics, Princeton University, Philips Medical Systems, Department of Biomedical Engineering, University of Rochester

Received June 8, 2006; E-mail: ivandmo@sas.upenn.edu

Abstract: Xenon-129 biosensors offer an attractive alternative to conventional MRI contrast agents due to the chemical shift sensitivity and large nuclear magnetic signal of hyperpolarized ^{129}Xe. Here, we report the first enzyme-responsive ^{129}Xe NMR biosensor. This compound was synthesized in 13 steps by attaching the consensus peptide substrate for matrix metalloproteinase-7 (MMP-7), an enzyme that is upregulated in many cancers, to the xenon-binding organic cage, cryptophane-A. The final coupling step was achieved on solid support in 80−92% yield via a copper (I)-catalyzed [3+2] cycloaddition. In vitro enzymatic cleavage assays were monitored by HPLC and fluorescence spectroscopy. The biosensor was determined to be an excellent substrate for MMP-7 ($K_M = 43\ \mu M$, $V_{max} = 1.3 \times 10^{-8}$ M s^{-1}, $k_{cat}/K_M = 7200$ M^{-1} s^{-1}). Enzymatic cleavage of the tryptophan-containing peptide led to a dramatic decrease in Trp fluorescence, $\lambda_{max} = 358$ nm. Stern−Volmer analysis gave an association constant of 9000 ± 1000 M^{-1} at 298 K between the cage and Trp-containing hexapeptide under enzymatic assay conditions. Most promisingly, ^{129}Xe NMR spectroscopy distinguished between the intact and cleaved biosensors with a 0.5 ppm difference in chemical shift. This difference most likely reflected a change in the electrostatic environment of ^{129}Xe, caused by the cleavage of three positively charged residues from the C-terminus. This work provides guidelines for the design and application of new enzyme-responsive ^{129}Xe NMR biosensors.

Introduction

Nuclear magnetic resonance (NMR) spectroscopy offers tremendous opportunities for high-resolution, minimally invasive, molecular imaging of deep tissue for the early diagnosis and treatment of disease. However, low sensitivity and complex background signals compromise biomarker detection. Recently, laser-polarized ^{129}Xe has gained attention as an MR probe,[1−5] due to its large signal (10−70% alignment of Xe nuclear spins, compared to thermal polarization of 0.00027% at 37 °C and 3 T) and wide NMR chemical-shift window (>200 ppm in water). Xenon gas is soluble in biological fluids (∼3.5 mM/atm at 37

°C),[6] nontoxic, and readily delivered by inhalation or perfusion. Furthermore, the environmental sensitivity of xenon chemical shift and relaxation parameters should allow the detection of multiple species in solution simultaneously.[7] Xenon represents, therefore, a useful probe for studying biological samples.[8] Important advances have been made by the Pines group and others, proving that ^{129}Xe NMR can report xenon−protein interactions.[9−11]

Xenon has been shown to bind cryptophane-A reversibly and with high affinity ($K_A = 3900$ M^{-1} at 278 K in C$_2$D$_2$Cl$_4$, K_A is higher in water). ^{129}Xe that is free in aqueous solution or bound inside the cage is distinguished by a greater than 120 ppm difference in ^{129}Xe NMR chemical shift. In order to couple ^{129}Xe chemical shifts with specific biological processes, Pines and Schultz exploited known methods for functionalizing the organic

† Department of Chemistry, University of Pennsylvania.
‡ Department of Physics, Princeton University.
§ Philips Medical Systems.
⊥ Department of Biomedical Engineering, University of Rochester.

(1) Mugler, J. P.; Driehuys, B.; Brookeman, J. R.; Cates, G. D.; Berr, S. S.; Bryant, R. G.; Daniel, T. M.; de Lange, E. E.; Downs, J. H.; Erickson, C. J.; Happer, W.; Hinton, D. P.; Kassel, N. F.; Maier, T.; Phillips, C. D.; Saam, B. T.; Sauer, K. L.; Wagshul, M. E. *Magn. Reson. Med.* **1997**, *37*, 809−815.
(2) Albert, M. S.; Cates, G. D.; Driehuys, B.; Happer, W.; Saam, B.; Springer, C. S.; Wishnia, A. *Nature* **1994**, *370*, 199−201.
(3) Bifone, A.; Song, Y. Q.; Seydoux, R.; Taylor, R. E.; Goodson, B. M.; Pietrass, T.; Budinger, T. F.; Navon, G.; Pines, A. *Proc. Natl. Acad. Sci. U.S.A.* **1996**, *93*, 12932−12936.
(4) Goodson, B. M.; Song, Y. Q.; Taylor, R. E.; Schepkin, V. D.; Brennan, K. M.; Chingas, G. C.; Budinger, T. F.; Navon, G.; Pines, A. *Proc. Natl. Acad. Sci. U.S.A.* **1997**, *94*, 14725−14729.
(5) Wolber, J.; McIntyre, D. J.; Rodrigues, L. M.; Carnochan, P.; Griffiths, J. R.; Leach, M. O.; Bifone, A. *Magn. Reson. Med.* **2001**, *46*, 586−591.

(6) Clever, L. H. *Krypton, Xenon, and Radon: Gas solubilities*; Pergamon Press: Oxford, 1979; Vol. 2, pp 1−357.
(7) Spence, M. M.; Rubin, S. M.; Dimitrov, I. E.; Ruiz, E. J.; Wemmer, D. E.; Pines, A.; Yao, S. Q.; Tian, F.; Schultz, P. G. *Proc. Natl. Acad. Sci. U.S.A.* **2001**, *98*, 10654−10657.
(8) Cherubini, A.; Bifone, A. *Prog. Nucl. Magn. Reson. Spectrosc.* **2003**, *42*, 1−30.
(9) Rubin, S. M.; Spence, M. M.; Goodson, B. M.; Wemmer, D. E.; Pines, A. *Proc. Natl. Acad. Sci. U.S.A.* **2000**, *97*, 9472−9475.
(10) Locci, E.; Dehouck, Y.; Casu, M.; Saba, G.; Lai, A.; Luhmer, M.; Reisse, J.; Bartik, K. *J. Magn. Reson.* **2001**, *150*, 167−174.
(11) Lowery, T. J.; Rubin, S. M.; Ruiz, E. J.; Spence, M. M.; Winssinger, N.; Schultz, P. G.; Pines, A.; Wemmer, D. E. *Magn. Reson. Imaging* **2003**, *21*, 1235−1239.
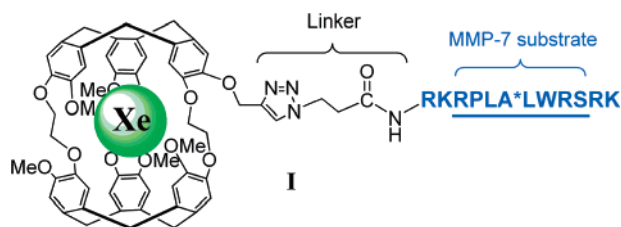
Figure 1. Structure of an MMP-7-responsive ^{129}Xe biosensor **I**, with xenon-binding cage, linker, and MMP-7-preferred peptide substrate (underlined in blue). Star indicates the enzyme cleavage site, while xenon (green sphere) is observed within the cage on the NMR time scale.

cage.[12,13] Attaching biotin to cryptophane-A created a variety of biosensors for streptavidin, whose binding produced as much as a 4 ppm change in ^{129}Xe chemical shift.[7,14−16] ^{129}Xe biosensors offer the possibility to functionalize various xenon-binding cages with different recognition units.[7,14−16] This work expands the range of accessible targets by describing the first enzyme-responsive ^{129}Xe NMR biosensor (compound **I**, Figure 1).

The design of enzyme-responsive MR contrast agents has been the focus of considerable recent research,[17,18] based on the goal of collecting biochemical information from optically dense tissues, such as tumors. Monitoring the catalytic activity of an enzyme, as opposed to stoichiometric protein binding, dramatically improves MR detection sensitivity, since a single enzyme can perform multiple, sometimes thousands, of turnovers. However, the design of such compounds has proven difficult, and there are still few examples.[19−29] One strategy involves modulating the coordination sphere of gadolinium, since water molecules that bind Gd(III) exhibit shorter T_1 relaxation times and enhanced ^{1}H NMR signals.[19−22] In one pioneering example, Meade et al. positioned a glucose molecule near Gd(III) in order to block water coordination until the sugar was cleaved by β-galactosidase.[20,21] However, it has proven

difficult to significantly and transiently alter the number of water molecules bound to Gd(III), and the abundance of water in biological samples gives high background signals. Furthermore, placing the substrate near the Gd(III) center imposes steric constraints on the enzyme and lowers catalytic efficiency.

Another high-relaxivity MR contrast agent is dextran-coated iron oxide. These superparamagnetic nanoparticles disrupt magnetic field homogeneity, which decreases T_2* signal from nearby water molecules. Researchers have demonstrated the detection of a single cell loaded with nanometer-sized iron oxide particles,[30] and even a single micrometer-sized iron oxide particle.[31] These particles appear to be nontoxic,[32] and Weissleder et al. demonstrated the use of iron oxide nanoparticles to detect DNA, proteins, and enzymatic activity,[23,25,27,28] where $1/T_2$ is directly proportional to nanoparticle cross-sectional area. However, changes in T_2 are too small for most in vivo applications,[27,28] and similarly to Gd(III), iron oxide agents offer few opportunities for multiplexed imaging, due to the difficulty of resolving multiple, different magnetic inhomogeneities within a complex biological sample.

Proteases serve as promising diagnostic indicators, based on their upregulation in many cancers.[33−35] The matrix metalloproteinases (MMPs), which degrade all components of the extracellular matrix and thereby influence a wide range of physiological and pathological processes, are particularly attractive candidates. For the design of an enzyme-responsive ^{129}Xe biosensor, we targeted MMP-7, based on its overexpression and extracellular localization in the progression of many tumors, particularly of the colon and breast.[33−35] This work complements various fluorogenic substrates that have been developed recently for imaging MMP-7 and other MMPs in tumors.[33,36,37]

In the present study, we describe an enzyme-responsive ^{129}Xe biosensor **I** in which an MMP-7 specific peptide substrate[33,38] was attached to cryptophane-A (Figure 1). This design was based on the sensitivity of encapsulated xenon for its local cage structure and remote environment, the varied charge of the biosensor molecule before (+5) and after (+2) MMP-7 cleavage, and the enzyme specificity imparted by the attached peptide recognition motif.[33,38] The synthesis was more efficient than the route described previously for cryptophanes functionalized with bioactive molecules.[7,14−16] The final step involved a stepwise Huisgen cycloaddition process:[39] copper (I)-catalyzed regioselective coupling of a peptide azide to a cryptophane-A terminal alkyne.[40,41] A fluorometric assay for MMP-7 activity

(12) Collet, A. *Tetrahedron* **1987**, *43*, 5725−5759.
(13) Bartik, K.; Luhmer, M.; Dutasta, J. P.; Collet, A.; Reisse, J. *J. Am. Chem. Soc.* **1998**, *120*, 784−791.
(14) Spence, M. M.; Ruiz, E. J.; Rubin, S. M.; Lowery, T. J.; Winssinger, N.; Schultz, P. G.; Wemmer, D. E.; Pines, A. *J. Am. Chem. Soc.* **2004**, *126*, 15287−15294.
(15) Hilty, C.; Lowery, T. J.; Wemmer, D. E.; Pines, A. *Angew. Chem., Int. Ed.* **2006**, *45*, 70−73.
(16) Lowery, T. J.; Garcia, S.; Chavez, L.; Ruiz, E. J.; Wu, T.; Brotin, T.; Dutasta, J. P.; King, D. S.; Schultz, P. G.; Pines, A.; Wemmer, D. E. *ChemBioChem* **2006**, *7*, 65−73.
(17) Lowe, M. P. *Aust. J. Chem.* **2002**, *55*, 551−556.
(18) Aime, S.; Cabella, C.; Colombatto, S.; Crich, S. G.; Gianolio, E.; Maggioni, F. *J. Magn. Reson. Imaging* **2002**, *16*, 394−406.
(19) Nivorozhkin, A. L.; Kolodziej, A. F.; Caravan, P.; Greenfield, M. T.; Lauffer, R. B.; McMurry, T. J. *Angew. Chem., Int. Ed.* **2001**, *40*, 2903−2906.
(20) Moats, R. A.; Fraser, S. E.; Meade, T. J. *Angew. Chem., Int. Ed. Engl.* **1997**, *36*, 726−728.
(21) Louie, A. Y.; Huber, M. M.; Ahrens, E. T.; Rothbacher, U.; Moats, R.; Jacobs, R. E.; Fraser, S. E.; Meade, T. J. *Nat. Biotechnol.* **2000**, *18*, 321−325.
(22) Duimstra, J. A.; Femia, F. J.; Meade, T. J. *J. Am. Chem. Soc.* **2005**, *127*, 12847−12855.
(23) Perez, J. M.; Josephson, L.; O'Loughlin, T.; Hogemann, D.; Weissleder, R. *Nat. Biotechnol.* **2002**, *20*, 816−820.
(24) Bogdanov, A.; Matuszewski, L.; Bremer, C.; Petrovsky, A.; Weissleder, R. *Mol. Imaging* **2002**, *1*, 16−23.
(25) Perez, J. M.; O'Loughin, T.; Simeone, F. J.; Weissleder, R.; Josephson, L. *J. Am. Chem. Soc.* **2002**, *124*, 2856−2857.
(26) Zhao, M.; Josephson, L.; Tang, Y.; Weissleder, R. *Angew. Chem., Int. Ed.* **2003**, *42*, 1375−1378.
(27) Perez, J. M.; Simeone, F. J.; Tsourkas, A.; Josephson, L.; Weissleder, R. *Nano Lett.* **2004**, *4*, 119−122.
(28) Perez, J. M.; Josephson, L.; Weissleder, R. *ChemBioChem* **2004**, *5*, 261−264.
(29) Querol, M.; Chen, J. W.; Weissleder, R.; Bogdanov, A. *Org. Lett.* **2005**, *7*, 1719−1722.

(30) Foster-Gareau, P.; Heyn, C.; Alejski, A.; Rutt, B. K. *Magn. Reson. Med.* **2003**, *49*, 968−971.
(31) Shapiro, E. M.; Skrtic, S.; Sharer, K.; Hill, J. M.; Dunbar, C. E.; Koretsky, A. P. *Proc. Natl. Acad. Sci. U.S.A.* **2004**, *101*, 10901−10906.
(32) Harisinghani, M. G.; Barentsz, J.; Hahn, P. F.; Deserno, W. M.; Tabatabaei, S.; van de Kaa, C. H.; de la Rosette, J.; Weissleder, R. *N. Engl. J. Med.* **2003**, *348*, 2491−2499.
(33) McIntyre, J. O.; Fingleton, B.; Wells, K. S.; Piston, D. W.; Lynch, C. C.; Gautam, S.; Matrisian, L. M. *Biochem. J.* **2004**, *377*, 617−628.
(34) Welch, A. R.; Holman, C. M.; Huber, M.; Brenner, M. C.; Browner, M. F.; VanWart, H. E. *Biochemistry* **1996**, *35*, 10103−10109.
(35) Yamashita, K.; Mori, M.; Shiraishi, T.; Shibuta, K.; Sugimachi, K. *Clin. Cancer Res.* **2000**, *6*, 1169−1174.
(36) Jiang, T.; Olson, E. S.; Nguyen, Q. T.; Roy, M.; Jennings, P. A.; Tsien, R. Y. *Proc. Natl. Acad. Sci. U.S.A.* **2004**, *101*, 17867−17872.
(37) Bremer, C.; Tung, C. H.; Weissleder, R. *Nat. Med.* **2001**, *7*, 743−748.
(38) Welch, A. R.; Holman, C. M.; Browner, M. F.; Gehring, M. R.; Kan, C. C.; VanWart, H. E. *Arch. Biochem. Biophys.* **1995**, *324*, 59−64.
(39) Padwa, A. *1,3-Dipolar Cycloaddition Chemistry;* Wiley: New York, 1984; pp 1−176.
(40) Punna, S.; Kuzelka, J.; Wang, Q.; Finn, M. G. *Angew. Chem., Int. Ed.* **2005**, *44*, 2215−2220.

Scheme 1. 12-Step Nonlinear Synthesis of Monopropargyl-Cryptophane-A
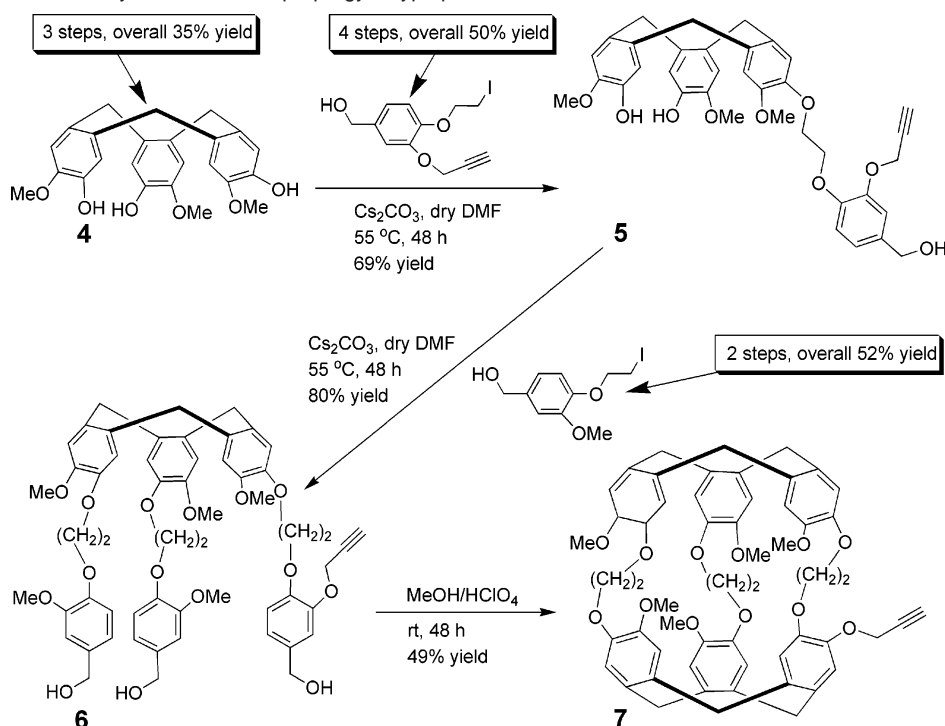
was developed to monitor the cleavage of the tryptophan-containing peptide fragment from the ^{129}Xe biosensor. Laser-polarized ^{129}Xe NMR spectroscopy showed a 0.5 ppm change in ^{129}Xe chemical shift between the intact biosensor and cleaved cryptophane product. This work illustrates important principles for the design and application of new enzyme-responsive ^{129}Xe NMR biosensors.

Experimental Procedures

Reagents. Organic reagents and solvents were used as purchased from the following commercial sources: *Sigma-Aldrich*: 3,4-dihydroxybenzaldehyde, sodium hydride, dimethyl sulfoxide (DMSO), dimethylformamide (DMF), methanol, triisopropylsilane (TIS), 2,6-lutidine, piperidine; *Acros*: propargyl bromide, dibromoethane; *Fisher*: tris(hydroxymethyl)aminomethane (Tris), calcium chloride, sodium chloride, copper(II) sulfate, sodium borohyride, sodium iodide, potassium carbonate, trifluoroacetic acid (TFA), diethyl ether (Et$_2$O), acetone, perchloric acid (60%); *Alfa Aesar*: cesium carbonate; *Novabiochem*: Fmoc-Lys(Boc)-Wang resin (0.67 mmol/g, 100−200 mesh), 2-(^{1}H-benzotriazole-1-yl)-1,1,3,3-tetramethyluronium hexafluorophosphate (HBTU), *N*-methylmorpholine (0.4 M), and Fmoc-protected amino acids Fmoc-L-Lys(Boc)-OH, Fmoc-L-Arg(Pbf)-OH, Fmoc-L-Ser-(*t*Bu)-OH, Fmoc-L-Ala-OH, Fmoc-L-Leu-OH, Fmoc-L-Pro-OH, Fmoc-L-Trp-OH); *BIOMOL International LP*: MMP-7 (recombinant, catalytic domain). For biological assays, all solutions were prepared using deionized water purified by Ultrapure Water Systems. The standard buffer is defined herein as 50 mM Tris, 5 mM CaCl$_2$, 300 mM NaCl, pH 7.5.

General Methods. All air- and moisture-sensitive reactions were performed under dinitrogen with glassware oven-dried and then flamed under partial vacuum. Peptides were generated using a Protein Technologies PS3 Peptide Synthesizer. HPLC analysis was performed on an Agilent 1100 system equipped with a quaternary pump and diode array detector using a Zorbax C-8 semipreparative (9.4 mm × 250 mm, 5 μm) or analytical column (4.6 mm × 150 mm, 5 μm). The

gradient eluent was composed of two solvents: 0.1% aqueous TFA (solvent A) and a 0.1% solution of TFA in CH$_3$CN (solvent B). Mass identification of all peptide-containing compounds was performed by the Wistar Institute Proteomics Facility using an Applied Biosystems Voyager 6030 MALDI-TOF mass spectrometer. ^{1}H (499.90 MHz) and ^{13}C (124.98 MHz) NMR spectra were obtained on a Brüker 500 MHz Fourier transform spectrometer at the University of Pennsylvania NMR facility, and recorded in CDCl$_3$ unless otherwise noted. The ^{1}H spectra were referenced to residual CHCl$_3$ (7.27 ppm). The ^{13}C spectra were referenced to the central line of CDCl$_3$ (77.23 ppm). ^{13}C and ^{1}H chemical shifts (δ) are given in parts per million (ppm) and reported to a precision of ± 0.01 ppm. Proton coupling constants (*J*) are given in Hz and reported to a precision of ± 0.1 Hz. Column chromatography was performed using 60 Å pore size, 40−75 μm particle size silica gel from Sorbent technologies. Thin layer chromatography (TLC) was performed using silica gel plates with UV light as the detection method.

Peptide Synthesis and Purification. Peptides N$_3$-CH$_2$CH$_2$-CONH$_2$-RKRPLALWRSRK, **1**; N$_3$-CH$_2$CH$_2$-CONH$_2$-RKRPLA, **2**; and LWRSRK, **3**, were synthesized using standard Fmoc amino acid protection chemistry on Fmoc-Lys(Boc)-Wang resin (0.1 mmol scale). Complete synthetic details are included in the Supporting Information. For purification of peptides **1**, **2**, and **3**, the following gradient was run: time 0, A/B = 90/10; 0−30 min, linear increase to A/B = 60/40; 30−32 min, linear change to A/B = 20/80; 32−42 min, A/B = 20/80. MALDI calculated for peptide **1**, C$_{73}$H$_{127}$N$_{30}$O$_{15}$ (M + H$^+$), 1664.01; found, 1663.72. MALDI calculated for peptide **2**, C$_{35}$H$_{65}$N$_{16}$O$_8$ (M + H$^+$), 836.95; found, 836.43. MALDI calculated for peptide **3**, C$_{38}$H$_{64}$N$_{14}$O$_8$ (M + H$^+$), 845.02; found, 845.28.

Organic Synthesis. Scheme 1 shows the synthetic route to monopropargyl-functionalized cryptophane-A, **7**.[42−45] The synthetic details for this compound are described in this section. The cyclotriguaiacylene,

(41) Rostovtsev, V. V.; Green, L. G.; Fokin, V. V.; Sharpless, K. B. *Angew. Chem., Int. Ed.* **2002**, *41*, 2596−2599.

(42) Brotin, T.; Lesage, A.; Emsley, L.; Collet, A. *J. Am. Chem. Soc.* **2000**, *122*, 1171−1174.
(43) Darzac, M.; Brotin, T.; Bouchu, D.; Dutasta, J. P. *Chem. Commun.* **2002**, 48−49.
(44) Brotin, T.; Barbe, R.; Darzac, M.; Dutasta, J. P. *Chem. Eur. J.* **2003**, *9*, 5784−5792.
(45) Darzac, M.; Brotin, T.; Rousset-Arzel, L.; Bouchu, D.; Dutasta, J. P. *New J. Chem.* **2004**, *28*, 502−512.

[3-propargyloxy-4-(2-iodoethoxy)phenyl]methanol linker, and [4-(2-iodoethoxy)-3-methoxyphenyl]methanol linker were prepared on the basis of reported syntheses of similar compounds.[42–48] Detailed synthetic procedures for these compounds are provided in the Supporting Information.

12-[2-(4-Hydroxymethyl-2-propargyloxyphenoxy)ethoxy]-3,8,13-trimethox-10,15-dihydro-5H-tribenzo[*a,d,g*]cyclononene-2,7-diol (5). To a two-neck flask with nitrogen inlet, cyclotriguaiacylene **4** (408 mg, 1 mmol, 1 equiv) and Cs_2CO_3 (975 mg, 3 mmol, 3 equiv) were added into anhydrous DMF (30 mL). The mixture was stirred at rt for 30 min. **[3-Propargyloxy-4-(2-iodoethoxy)phenyl]methanol** (331 mg, 1 mmol, 1 equiv) was then added in one portion, and the resulting mixture was heated at 55 °C for 48 h under N_2 atmosphere. The mixture was poured into water (200 mL), and the product was extracted with ethyl acetate. The combined organic extracts were concentrated to 200 mL and washed subsequently with NaOH (3 × 200 mL), water (200 mL), and brine (5 × 200 mL). The organic layer was dried over $MgSO_4$ and filtered, and the solvent was removed under vacuum. The crude product as a brownish solid was chromatographed on a silica gel column (eluent: 1 to 3% methanol in CH_2Cl_2) to give pure product as a white solid (420 mg, yield: 69%). ^{1}H NMR δ = 6.98 (s, 1H), 6.90 (s, 1H), 6.84 (t, *J* = 5.8, 3H), 6.77 (s, 1H), 6.72 (d, *J* = 2.3, 2H), 4.64 (two doublets, *J* = 13.7, *J* = 14.3, 3H), 4.58 (d, *J* = 2.3, 2H, $-OCH_2C\equiv$CH), 4.54 (s, 2H, $-CH_2OH$), 4.30 (m, 4H, $-OCH_2CH_2O-$), 3.76 (s, 3H, $-OCH_3$), 3.75 (s, 3H, $-OCH_3$), 3.66 (s, 3H, $-OCH_3$), 3.44 (two doublets, *J* = 13.7, *J* = 13.5, 3H), 2.41 (t, *J* = 2.3, 1H, $-C\equiv$CH). ^{13}C NMR δ = 148.59, 148.42, 147.41, 146.62, 145.40, 144.19, 144.17, 134.39, 133.28, 132.63, 132.30, 132.10, 131.41, 131.32, 121.14, 116.80, 115.79, 115.67, 114.61, 114.29, 113.84, 112.32, 78.91, 75.92, 68.18, 67.84, 65.08, 56.99, 56.25, 56.16, 56.10, 36.44, 36.34, 36.30. HRMS calculated for $C_{36}H_{36}O_9$ (M + Na^+), 635.2257; found, 635.2232.

{3-Propargyloxy-4-[2-(3,8,13-trimethoxy-7,12-bis[2-(4-hydryoxymethyl-2-methoxyphenoxy)ethoxy]-10,15-dihydro-5H-tribenzo-[*a,d,g*]cyclononen-2-yloxy)ethoxy] phenyl}methanol (6). According to the procedure for the synthesis of **5**, compound **6** (700 mg, yield: 80%) was obtained from the reaction of **5** (560 mg, 0.91 mmol, 1 equiv), **[4-(2-iodoethoxy)-3-methoxyphenyl]methanol** (800 mg, 2.7 mmol, 3 equiv), and Cs_2CO_3 (1.2 g, 3.7 mmol, 4 equiv) in anhydrous DMF (20 mL). ^{1}H NMR δ = 7.01–6.80 (m, 15H), 4.73 (d, *J* = 13.7, 3H), 4.61 (m, 8H), 4.38 (m, 4H, $-OCH_2CH_2O-$), 3.75 (s, 3H, $-OCH_3$), 3.74 (s, 3H, $-OCH_3$), 3.69 (s, 9H, $-OCH_3$), 3.53 (d, *J* = 13.7, 3H, $-OCH_3$), 2.45 (d, *J* = 2.3, 1H, $-C\equiv$CH). ^{13}C NMR δ = 149.73, 148.61, 148.55, 148.50, 148.31, 147.52, 147.51, 147.50, 146.89, 146.88, 146.82, 134.74, 133.21, 133.14, 131.99, 121.13, 119.54, 116.73, 116.60, 116.59, 114.59, 114.55, 113.86, 111.05, 78.90, 75.97, 68.17, 67.98, 67.80, 65.28, 65.08, 56.96, 56.27, 56.23, 55.90, 36.56. HRMS calculated for $C_{56}H_{60}O_{15}$ (M + Na^+), 995.3829; found, 995.3808.

Monopropargyl-Cryptophane-A (7). Methanol (150 mL) was added to a stirred solution of **6** (90 mg, 0.09 mmol) in CH_2Cl_2 (10 mL). Perchloric acid (150 mL) was then added dropwise into the cloudy solution at 0 °C. The reaction was allowed to warm to rt and stirred slowly for 48 h under N_2. The reaction mixture was diluted by CH_2Cl_2 (300 mL) and neutralized by 1 M NaOH solution at 0 °C. The CH_2Cl_2 and aqueous phases were separated, and the aqueous layer was extracted with CH_2Cl_2 (3 × 250 mL). The combined organic extracts were concentrated to 300 mL and washed with $NaHCO_3$ solution and brine several times. The solution was filtered and dried over $MgSO_4$. After removal of the solvent under vacuum, the brownish residue was chromatographed on a silica gel column (eluent: 1 to 3% methanol in CH_2Cl_2) to give pure product as a light yellowish solid (42 mg, yield: 49%). ^{1}H NMR δ = 6.90 (s, 2H), 6.78 (s, 2H), 6.76 (s, 4H), 6.69 (t,

(46) Brotin, T.; Devic, T.; Lesage, A.; Emsley, L.; Collet, A. *Chem. Eur. J.* **2001**, *7*, 1561–1573.
(47) Canceill, J.; Collet, A.; Gottarelli, G. *J. Am. Chem. Soc.* **1984**, *106*, 5997–6003.
(48) Canceill, J.; Lacombe, L.; Collet, A. *J. Am. Chem. Soc.* **1985**, *107*, 6993–6996.

Scheme 2. Synthesis of Biosensors **I** and **II** with the Final Step Involving Cu(I)-Catalyzed Cycloaddition of Monopropargyl-Cryptophane-A to Azidopeptide on Solid Support[a]
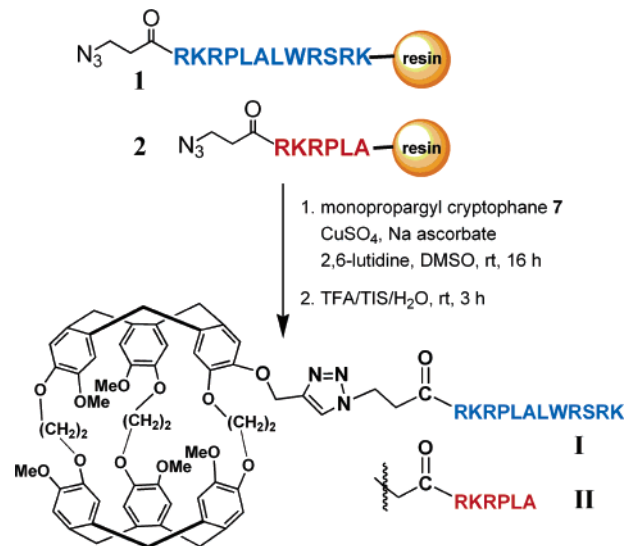
[a] Reaction of **1** or **2** with **7**, followed by TFA cleavage and HPLC purification, yielded **I** and **II** in 80–92% yield.

J = 5.0, 4H), 4.72 (dd, J_1 = 3.2, J_2 = 21.6, 3H), 4.61 (d, *J* = 18.2, 5H), 4.18 (m, 12H, $-OCH_2CH_2O-$), 3.81 (s, 5H, $-OCH_3$), 3.80 (s, 5H, $-OCH_3$), 3.78 (s, 5H, $-OCH_3$), 3.42 (d, *J* = 19.2, 6H), 2.70 (t, *J* = 3.2, 1H, $-C\equiv$CH). ^{13}C NMR δ = 150.46, 150.43, 150.28, 148.57, 148.00, 147.39, 147.27, 135.06, 134.88, 134.83, 134.76, 134.48, 133.89, 132.44, 132.29, 132.24, 132.16, 122.30, 122.19, 121.96, 121.30, 121.19, 121.14, 118.08, 114.69, 114.48, 114.40, 114.33, 79.65, 76.82, 70.27 ($-OCH_2CH_2O-$), 70.17 ($-OCH_2CH_2O-$), 69.92 ($-OCH_2CH_2O-$), 69.89 ($-OCH_2CH_2O-$), 58.01 ($-OCH_2C\equiv$CH), 56.83 ($-OCH_3$), 56.46 ($-OCH_3$), 56.38 ($-OCH_3$), 56.26 ($-OCH_3$), 36.88 ($-CH_2-$). HRMS calculated for $C_{56}H_{54}O_{12}$ (M + Na^+) 941.3513; found, 941.3541.

[3 + 2] Cycloaddition. As shown in Scheme 2, a solution of copper(II) sulfate (0.006 mmol, 0.5 equiv) was added to the azidopeptide-modified resin (20 mg, maximum 0.0124 mmol azidopeptide **1** or **2**, 1 equiv) followed by 2,6-lutidine (2.78 μL, 0.024 mmol, 2 equiv), sodium ascorbate (0.018 mmol, 1.5 equiv), and monopropargyl-cryptophane-A **7** (21 mg, 0.024 mmol, 2 equiv). The suspension was degassed with gentle N_2 flow and stirred at rt for 16 h. The resin was transferred to a fritted reaction vessel and washed sequentially with CH_2Cl_2, MeOH, water, and 1:1 MeOH:CH_2Cl_2. The resin was then dried under vacuum.

Cleavage of the conjugate product from the resin was accomplished by treating the dried resin at rt for 3 h with a mixture of TFA, water, thioanisole, phenol, ethanedithiol, and triisopropylsilane (81.5/5/5/5/2.5/1) for peptide containing unprotected Trp and with TFA, water, and triisopropylsilane (95/2.5/2.5) for peptide without the Trp residue. The resin was removed by filtration and rinsed with minimal TFA. Addition of anhydrous Et_2O to the filtrate gave a white solid precipitate, which was washed with anhydrous Et_2O, collected by centrifugation and dried under vacuum to yield crude product. The products **I** and **II** were purified by HPLC with the following gradient: time 0, A/B = 75/25; 0–30 min, linear increase to A/B = 45/55; 30–32 min, linear change to A/B = 20/80; 32–42 min, A/B = 20/80. MALDI calculated for intact biosensor **I**, $C_{129}H_{181}N_{30}O_{27}$ (M + H^+), 2582.37; found, 2582.42. MALDI calculated for cleaved biosensor **II**, $C_{91}H_{119}N_{16}O_{20}$ (M + H^+), 1756.31; found, 1756.64.

Enzymatic Assay, Monitored by HPLC. At rt, an aliquot (2 μL) of active MMP-7 (0.454 μg/μL) was added into 0.998 mL of a freshly prepared solution of biosensor **I** at a known concentration in standard buffer. The extinction coefficient of **I**, ϵ = 15,000 M^{-1} cm^{-1} at 280 nm in water, was determined from a solution containing the weighed

sample. At approximately 3 min intervals, 70 μL aliquots were removed from the reaction mixture and immediately quenched with 30 μL of a 40 mM EDTA solution. Each aliquot was analyzed by HPLC with the gradient: time 0, A/B = 75/25; 0–30 min, linear increase to A/B = 45/55; 30–32 min, linear change to A/B = 20/80; 32–42 min, A/B = 20/80. The retention times for **I** and **II** were 15.6 and 17.9 min, respectively. The enzyme activity was determined from the initial rate of increase in the concentration of cleaved sensor **II**, during the consumption of the first 10–15% of substrate **I**. The absorbance at 280 nm of the growing peak at 17.9 min was integrated and compared for each time point. Initial velocities were measured at substrate **I** concentrations of 6, 16, 28, 38, 48, 74, and 100 μM.

The k_{cat}/K_M value for all peptide substrates was calculated on the basis of the Michaelis–Menten equation (eq 1) after fitting the activity data at varying substrate concentrations with a nonlinear regression curve:

$$\nu = \frac{[E]_0[S]k_{cat}}{K_M + [S]} \tag{1}$$

where $[E]_0$ and $[S]$ were the total enzyme and substrate concentrations in solution, k_{cat} was the rate of product formation by the enzyme–substrate complex, and K_M was the Michaelis constant, which gave the concentration of substrate at which the reaction occurred at half of the maximum rate, V_{max}.

For the azidopeptide substrate **1**, enzyme activity was determined similarly by HPLC with the gradient: time 0, A/B = 90/10; 0–30 min, linear increase to A/B = 60/40; 30–32 min, linear change to A/B = 20/80; 32–42 min, A/B = 20/80. Peak areas were monitored for the intact substrate **1** and cleaved hexapeptide product **3** at retention times of 17.0 and 10.3 min, respectively. Initial velocities were measured at substrate **1** concentrations of 6, 50, 100, and 870 μM.

Fluorescence Spectroscopy and Fluorometric Enzymatic Assay. Fluorescence spectra of **I** and **II** dissolved in standard buffer (λ_{ex} = 295 nm) were measured in small volume, 1-cm path length quartz cuvettes at 298 K using a Varian Cary Eclipse fluorescence spectrophotometer operated with the Cary Eclipse Bio software package (1 nm steps, 5 nm excitation and emission slits). Kinetics data were collected at 30 s intervals using the same software on samples with controlled temperature and stirring.

For the fluorometric enzymatic assay, an aliquot (2 μL) of active MMP-7 (0.454 μg/μL) was added into 0.998 mL solution of ^{129}Xe biosensor **I** with known concentration at 298 K. Fluorescence spectra were collected from 310–450 nm. All reported fluorescence data are uncorrected and are roughly 5 nm red-shifted from the values obtained when the instrumental correction feature is employed. Trp fluorescence at 400 nm was analyzed as a function of time, since there was little contribution at this wavelength from monopropargyl-cryptophane-A fluorescence. The enzyme activity was calculated from the initial rate of decrease in Trp emission at 400 nm, over the time interval that corresponded to the first 10–15% completion of the reaction. The k_{cat}/K_M value for biosensor **I** was calculated by nonlinear regression of the activity data by varying the biosensor concentration from 6–100 μM; double-reciprocal $1/\nu$ versus $1/[S]$ Lineweaver–Burk plots[49] gave a similar k_{cat}/K_M value.

^{129}Xe NMR Spectroscopy. ^{129}Xe chemical shift data for **I** and **II** were collected in D$_2$O solution on a homemade spectrometer[50] connected to a home-built ^{129}Xe probe mounted in the bore of an Oxford 9.4 T magnet (^{1}H = 400 MHz). Isotopically enriched xenon (86% ^{129}Xe and 0.13% ^{131}Xe, Spectra Gases) was polarized and cryogenically separated from the buffer–gas mixture in a Nycomed-Amersham (now GE) IGI.Xe.2000 polarizer (output polarization 10–20%) and then quickly transferred to a special aluminum container inside the ^{129}Xe probe. At 9.4 T, the spin relaxation time T_1 of ^{129}Xe gas in the container ranged from 70 to 120 min. A 5 mm sample test tube and an NMR tank circuit, along with the output gas capillary, were mounted on a removable probe insert, a configuration which allowed the sample to be changed without removing the hyperpolarized xenon container from the magnet bore. Sample temperature (unregulated) in the probe was stable at 18 ± 1 °C, whereas the solutions were prepared at rt, 23 ± 1 °C. This difference in temperature led to an initial cooling of the sample upon introduction into the probe, and the sample was allowed to sit to achieve thermal equilibrium with the probe. By opening a needle valve mounted on the container and monitoring the output gas flow rate, pure hyperpolarized xenon gas was gently bubbled through the test tube containing the sample solution; then the bubbling was stopped, and NMR scans (n = 1–32, ^{129}Xe frequency 110.45 MHz, 10–30° tipping pulse) were performed and averaged. Raw free induction decay (FID) signals were recorded in quadrature, then processed using standard baseline and phase corrections, fast Fourier transform, and Gaussian broadening of 20 Hz. Peaks attributed to gaseous xenon at 1 atm inside the input capillary (coaxial with the vertical sample tube) were taken as +0.55 ppm frequency reference,[51] making the observed peaks consistent with the published data for ^{129}Xe dissolved in pure D$_2$O[52] and in cryptophanes,[13,14,42] after taking into account the temperature dependence of the frequency shifts.[13,14,42] All curve fitting was performed with IGOR Pro 5 (WaveMetrics, Inc., Oregon) prior to applying Gaussian broadening. The uncertainties in ^{129}Xe chemical shifts from peak fits were small ($\sim$2 Hz, 0.02 ppm), with additional sources of error (such as assignment of the gas reference peak) being much less than the linewidths of approximately 20 Hz. These contributions resulted in peak uncertainties of approximately ±0.05 ppm. ^{129}Xe chemical shifts are reported to a precision of ±0.1 ppm.

Results

Synthesis of Peptide–Cryptophane-A Conjugates. In designing biosensor **I**, the sequence RPLALWRS was chosen because of the high specificity of MMP-7 for this substrate and its successful function in a fluorogenic beacon for in vivo detection and imaging of MMP-7.[33,38] Schemes 1 and 2 outline the synthesis of **I**. Cryptophane-A was synthesized with a single propargyl group, which not only overcame the hurdles of allyl ether deprotection and subsequent low-yielding alkylation that confronted previous studies with cryptophanol,[7,14,43,45] but also provided an efficient route to couple a variety of peptides to cryptophane-A via azide-alkyne [3 + 2] cycloaddition.[40,41] **II** was generated through two different methods: (a) MMP-7-mediated enzymatic hydrolysis of **I** and (b) direct synthesis on solid support, as described (Scheme 2). Both routes gave the desired product, as confirmed by HPLC and MALDI-TOF mass spectrometry. The latter method was more efficient in generating large quantities of material for this study.

Monopropargylated cryptophane-A **7** was synthesized in 12 nonlinear steps by following a modified template method which involved stepwise incorporation of two types of linkers and the formation of two cyclotriveratrylene units in two different stages of synthesis.[12] Starting from vanillyl alcohol, cyclotriguaiacylene **4** was prepared in three steps and 35% overall yield, based on a known procedure.[12,42–48] Two linkers were synthesized for attachment to **4**: [3-propargyloxy-4-(2-iodoethoxy)phenyl]-methanol (4 steps, 49% yield) and [4-(2-iodoethoxy)-3-meth-

(49) Segel, I. H. *Enzyme Kinetics: Behavior and Analysis of Rapid Equilibrium and Steady-State Enzyme Systems*; John Wiley & Sons: New York, 1993; pp 1–957.

(50) Patton, B.; Kuzma, N. N.; Happer, W. *Phys. Rev. B* **2002**, *65*, 020404.

(51) Jameson, C. J.; Jameson, A. K.; Cohen, S. M. *J. Chem. Phys.* **1973**, *59*, 4540–4546.

(52) Grishin, Y. K.; Mazitov, R. K.; Panov, A. N. *Appl. Magn. Reson.* **1998**, *14*, 357–366.
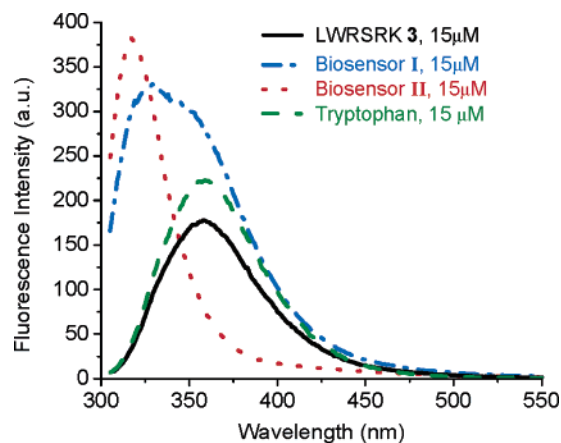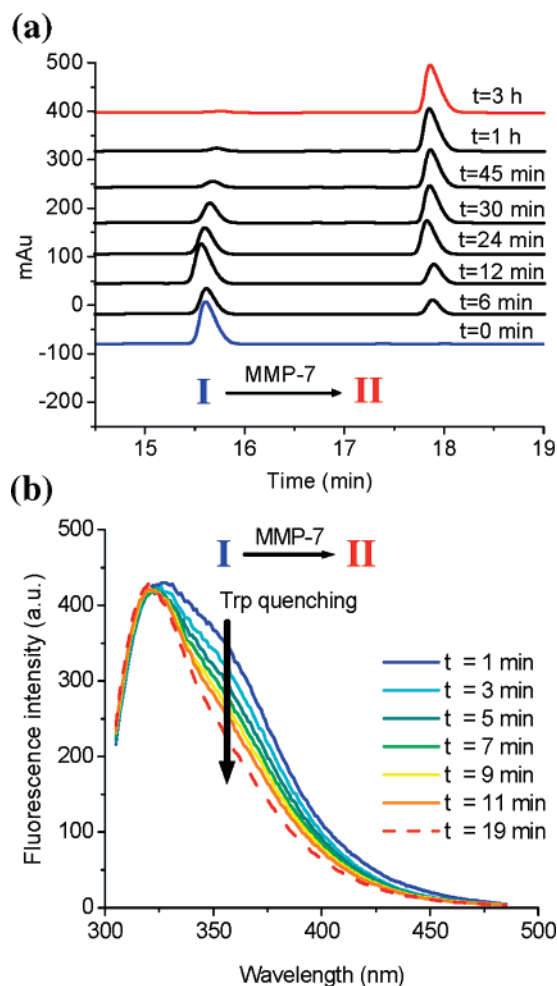
Figure 2. Fluorescence spectra of biosensor **I**, cleaved biosensor **II**, hexapeptide LWRSRK **3**, and tryptophan. All spectra were obtained by excitation at 295 nm at rt in standard buffer.

oxyphenyl]methanol (2 steps, 52% yield). In the presence of cesium carbonate as base, **4** was alkylated with one [3-propargyloxy-4-(2-iodoethoxy)phenyl]methanol linker, followed by two [4-(2-iodoethoxy)-3-methoxyphenyl]methanol linkers, to give precursor **6** in 50−55% yield for the two alkylation steps. As compared with literature reports of 15−25%,[42−45] substantially improved yields of alkylation were achieved with lower reaction temperatures and longer reaction times. The most challenging step was the cyclization of precursor **6** to afford **7**. This had been reported to be low yielding in the synthesis of other monofunctionalized cryptophane-A compounds.[43] Several trials on the final cyclization using pure formic acid or a chloroform/formic acid mixture (50/50) at 55 °C led to multiple non-isolable compounds, with very little product appearing on TLC. However, the desired cyclized product **7** was obtained in 49% yield by using perchloric acid/MeOH (50/50) at rt. Further attempts using perchloric acid/MeOH mixtures at elevated temperatures led to decomposition of starting material.

The azidopeptides N_3-CH$_2$CH$_2$-CONH$_2$-RKRPLALWRSRK, **1**, and N_3-CH$_2$CH$_2$-CONH$_2$-RKRPLA, **2**, were synthesized by standard solid-phase synthesis using Fmoc-substituted reagents.[53] 3-Azido propionic acid was prepared according to literature procedures[54] and incorporated as the N-terminal residue. Yields of purified peptides were about 80% for all peptide coupling and cleavage steps, based on the maximum possible yield from the amount of starting resin. While still attached to the Wang resin, the azidopeptide was coupled to the monopropargyl-cryptophane-A by a copper (I)-catalyzed [3 + 2] cycloaddition to give biosensor in 80−92% yield.[40,41] After cleavage from solid support, reversed phase HPLC analysis showed complete disappearance of azidopeptide and appearance of new peaks at longer retention times, as expected for peptides conjugated to the hydrophobic cryptophane. Pooled fractions for each product were collected and lyophilized, and all compounds were characterized by MALDI-TOF mass spectrometry. Figure 2 shows the emission spectra for the intact cryptophane sensor **I**, cleaved cryptophane sensor **II**, LWRSRK **3**, and free tryptophan.

Enzymatic Assay. The ability of MMP-7 to hydrolyze ^{129}Xe biosensor **I** was initially confirmed by HPLC analysis (Figure

(53) Atherton, E.; Sheppard, R. C. *Solid-Phase Peptide Synthesis*; IRL Press: Oxford, 1989; pp 1−203.
(54) Leffler, J. E.; Temple, R. D. *J. Am. Chem. Soc.* **1967**, *89*, 5235−5246.
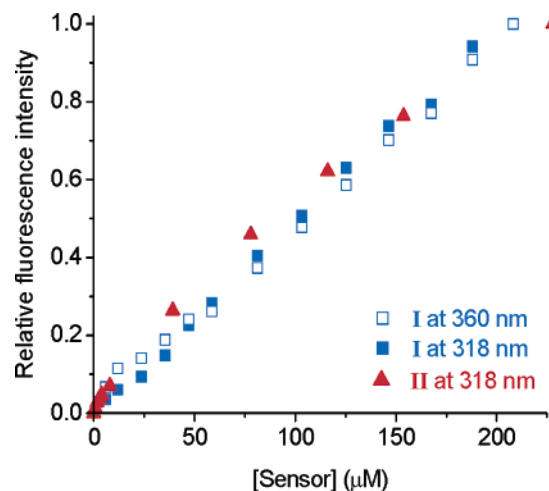
Figure 3. (a) HPLC traces for aliquots of biosensor **I** (32 μM) digested by MMP-7 (42 nM) at rt in standard buffer to give **II**. Proteolysis was stopped at the indicated time points by EDTA addition, then analyzed by reversed phase HPLC. (b) Fluorometry monitored digestion of biosensor **I** (32 μM) by MMP-7 (42 nM) at rt in standard buffer. Trp fluorescence (λ_{ex} = 295 nm, λ_{em} = 358 nm) decreased during the reaction.

3a). A standard assay was performed by incubating a 1 mL reaction mixture of 32 nmol **I** and 42 pmol MMP-7 at 310 K. Reaction progress was monitored by analyzing aliquots of the reaction mixture at regular intervals. HPLC data showed a progressive decrease of the intact biosensor **I** at retention time of 15.6 min and a concomitant increase of two new peaks at retention times of 3.0 min and 17.9 min. MALDI-TOF mass spectrometry identified these new peaks as the cleaved hexapeptide LWRSRK **3** and cryptophane−peptide product **II**, respectively. The peptide cleavage pattern agreed with previous assays using this substrate.[33,34,38] The 2.3-min increase in retention time was consistent with the lower charge of the cleaved product **II** (+2) relative to the intact biosensor **I** (+5).

Biosensor **I** contained a single tryptophan near the C-terminus that was two residues removed from the cleavage site for MMP-7. Considering the sensitivity of Trp fluorescence to its environment, we explored whether the Trp emission changed upon peptide cleavage. The broad fluorescence spectrum of **I** (Figure 2) was assigned to contributions from both cryptophane-A (λ_{max} = 318 nm) and Trp (λ_{max} = 358 nm). The Trp fluorescence spectra of **I** and **3** were red-shifted, as is typical

Table 1. Comparison of MMP-7 Activity toward **I**, Monitored by UV−vis (HPLC) and Fluorometry

	biosensor **I** (μM)		
	6	50	100
	Initial Velocity (pmol/s)		
HPLC assay	1	10	7
fluorometric assay	0.9	9	8

for the fully solvated amino acid in pH 7.5 water.[55] The fluorescence spectrum of **3** was diminished from free tryptophan in solution (Figure 2), indicating considerable Trp quenching in the environment of the hexapeptide. There are no other aromatic residues within the hexapeptide that would contribute to quenching by energy transfer, but quenching of tryptophan by excited-state proton and electron transfer is well-known within peptides and proteins.[55]

In enzyme kinetics studies, the fluorescence spectrum of **I** was taken at 30 s intervals after addition of MMP-7 (Figure 3b). A continuous decrease of Trp emission was observed that was attributed to the aforementioned intramolecular quenching processes. A similar decrease in Trp fluorescence intensity was observed upon cleavage of peptide **1** (data not shown). The change in fluorescence intensity at 400 nm was used to calculate the initial velocity (v) of the enzyme reaction. The v values determined by HPLC and fluorometric methods were in excellent agreement (Table 1), which validated using the fluorometric assay to monitor this enzyme reaction. The Trp fluorescence assays were easier to run, allowed continuous monitoring of the reaction, provided greater sensitivity, and required less material than HPLC-based UV−vis absorbance measurements.

Fluorescence Studies. Experiments were performed to investigate Trp fluoresence under different experimental conditions. In the fully extended biosensor **I** (Figure 1) cryptophane and Trp were separated by approximately 40 Å. Temperature dependence studies identified little contribution to Trp quenching from the cryptophane within the intact biosensor **I** (see Supporting Information). The observed decrease in Trp fluorescence at elevated temperatures (λ_{em} = 358 nm, F/F_0 = 0.3 at 353 K) was virtually identical to that seen with the Trp-containing hexapeptide **3**, and was thus attributed to temperature-dependent solvent quenching by nonradiative decay processes.[56] The similar fluorescence temperature dependence for **I** and **3** also suggested a lack of intermolecular interactions between biosensors, since higher temperatures should dissociate any aggregates in solution. This was confirmed with **I** and **II** by comparing the concentration dependence of fluorescence intensity (λ_{ex} = 295 nm, λ_{em} = 318 nm for cryptophane, and λ_{em} = 358 nm for Trp), after correcting for inner filter effects and dilution.[55] Neither compound's fluorescence intensity deviated from linearity over the concentration range, 1−250 μM (Figure 4). The absorption and fluorescence maxima were unchanged over this range (data not shown). The biosensors were very soluble in water, and the fluorescence studies indicated that **I**, **II**, and related amphiphilic cryptophanes were unlikely to aggregate at concentrations relevant to the present ^{129}Xe NMR studies.

(55) Lakowicz, J. R. *Principles of Fluorescence Spectroscopy,* 2nd ed.; Kluwer Academic/Plenum: New York, 1999; pp 237−259.
(56) Chen, Y.; Barkley, M. D. *Biochemistry* **1998**, *37*, 9976−9982.

Figure 4. Concentration dependence of biosensor fluorescence intensity (**I** and **II**, λ_{ex} = 295 nm, λ_{em} monitored at 318 or 358 nm, corresponding to emission from cryptophane and Trp, respectively). Solutions at rt in standard buffer. The fluorescence intensity for each compound at a given wavelength and concentration was normalized to its value at the maximum biosensor concentration, in order to facilitate comparison and show linearity over a large concentration range.
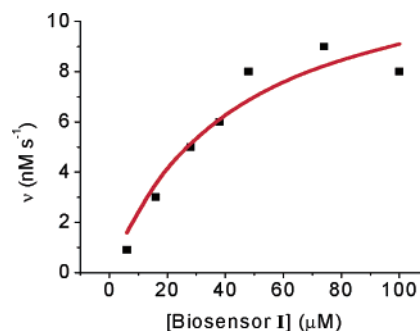
Having ruled out a prevalent role for intra- and intermolecular interactions within or between biosensors, we sought further to investigate whether the cryptophane contributed to the observed decrease in Trp fluorescence upon enzymatic cleavage. The quenching process observed in the MMP-7 cleavage assay was very efficient, which discounted the possibility of diffusion-controlled bimolecular collisional quenching ($k_q \approx 10^9$ M^{-1} s^{-1}), based on the low micromolar concentrations of (equimolar) Trp and cryptophane, and short lifetime of the Trp excited state ($\sim10^{-8}$ s).[55] Thus, it was investigated whether static quenching caused by association between the Trp-containing hexapeptide, LWRSRK **3**, and cryptophane, could occur. To examine this possible quenching mechanism, the steady-state fluorescence intensity of the hexapeptide LWRSRK **3** was measured as a function of the cleaved sensor **II** (putative quencher) concentration in standard buffer. This Stern−Volmer experiment could only be performed within a limited range of **II** concentrations, due to limitations in the quantity of material and the contribution of this compound to total fluorescence. Nonetheless, 8-fold excess quencher was sufficient to elucidate the strength of the cryptophane−hexapeptide interaction. All fluorescence spectra were corrected to remove contributions from cryptophane. Considerable absorbance at 280 nm from the cryptophane, coupled with residual cryptophane fluoresence intensity even after correction, compromised the quality of these data. The resulting fluorescence maximum at 358 nm, which mainly corresponded to Trp emission of **I**, decreased with successive additions of **II**. The slope of F_0/F vs [**II**] gave the association constant, K_S = 9000 ± 1000 M^{-1}, for the formation of a nonfluorescent ground-state complex between Trp and cryptophane (Figure 5).[55] The Stern−Volmer experiment revealed strong Trp−cryptophane complex formation, leading to a loss of Trp fluorescence. Within this concentration range, there was no significant deviation from linearity that indicated additional contributions from collisional quenching processes.

Cryptophanes are known to encapsulate some cationic molecules with high affinity ($K_A \approx 2700$−6400 M^{-1}) due to
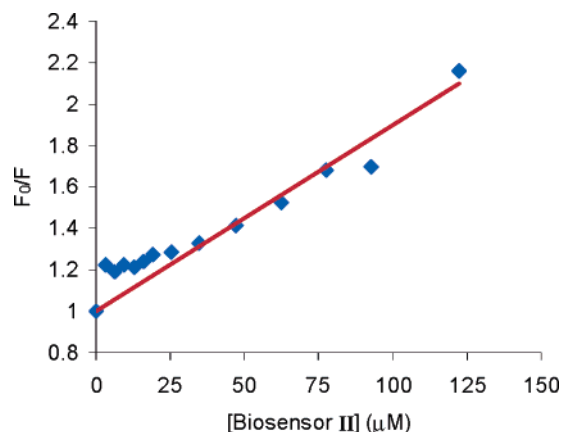
Figure 5. Stern−Volmer plot of fluorescence quenching of Trp-containing hexapeptide **3** (16 μM, 298 K in standard buffer) by cleaved biosensor **II**. Solution of **3** was titrated with 3.18 mM **II**, to achieve concentrations of **II** between 0 and 120 μM. Steady-state fluorescence measurements found the ratio of initial fluorescence, F_0, to observed fluorescence, F, at each quencher concentration. The linear fit gave an R^2 value of 0.88, which indicated a dominant static quenching mechanism. The slope of this line gave the association constant, $K_S = 9000$ M^{-1}, for the **II-3** complex.

both cation-π and hydrophobic interactions;[57,58] thus, comparable association between electron-rich cryptophane and the positively charged peptide could be responsible for stable complex formation. Trp is known to function as an efficient quencher for some organic dyes via photoinduced electron transfer, and Trp emission can be quenched by Tyr and Phe via long-range energy transfer.[59−63] The limited spectral overlap between cryptophane emission and Trp absorption reduced possibilities for long-range fluorescence energy transfer, as evidenced by the lack of Trp quenching that was observed within the intact biosensor **I**. Alternatively, the observed Trp quenching could involve a shorter-range, photoinduced electron-transfer reaction between Trp and cryptophane-A. However, cryptophane-A (reversible oxidation at 0.69 V for related cryptophane-E in acetonitrile with Ag/AgNO$_3$ reference electrode)[64] and tryptophan (midpoint potential = 1.02 V vs NHE at pH 7)[65] are both good reducing agents, and formation of the Trp radical cation by electron transfer was disfavored thermodynamically. More simply, π-stacking between tryptophan and the cryptophane could mediate this interaction and lead to quenched Trp fluorescence, as has been observed in many previous studies.[62,66−68] However, we have no direct spectroscopic evidence of π-stacking interactions at this time. We are currently

(57) Garel, L.; Lozach, B.; Dutasta, J. P.; Collet, A. *J. Am. Chem. Soc.* **1993**, *115*, 11652−11653.
(58) Garcia, C.; Humiliere, D.; Riva, N.; Collet, A.; Dutasta, J. P. *Org. Biomol. Chem.* **2003**, *1*, 2207−2216.
(59) Jones, G.; Lu, L. N.; Vullev, V.; Gosztola, D. J.; Greenfield, S. R.; Wasielewski, M. R. *Bioorg. Med. Chem. Lett.* **1995**, *5*, 2385−2390.
(60) Neuweiler, H.; Schulz, A.; Bohmer, M.; Enderlein, J.; Sauer, M. *J. Am. Chem. Soc.* **2003**, *125*, 5324−5330.
(61) Wagenknecht, H. A.; Stemp, E. D. A.; Barton, J. K. *J. Am. Chem. Soc.* **2000**, *122*, 1−7.
(62) Bush, M. E.; Bouley, N. D.; Urbach, A. R. *J. Am. Chem. Soc.* **2005**, *127*, 14511−14517.
(63) Marme, N.; Knemeyer, J. P.; Wolfrum, J.; Sauer, M. *Angew. Chem., Int. Ed.* **2004**, *43*, 3798−3801.
(64) Renault, A.; Talham, D.; Canceill, J.; Batail, P.; Collet, A.; Lajzerowicz, J. *Angew. Chem., Int. Ed. Engl.* **1989**, *28*, 1249−1250.
(65) DeFelippis, M. R.; Murthy, C. P.; Broitman, F.; Weinraub, D.; Faraggi, M.; Klapper, M. H. *J. Phys. Chem.* **1991**, *95*, 3416−3419.
(66) Marme, N.; Knemeyer, J. P.; Sauer, M.; Wolfrum, J. *Bioconjugate Chem.* **2003**, *14*, 1133−1139.
(67) Vaiana, A. C.; Neuweiler, H.; Schulz, A.; Wolfrum, J.; Sauer, M.; Smith, J. C. *J. Am. Chem. Soc.* **2003**, *125*, 14564−14572.
(68) Doose, S.; Neuweiler, H.; Sauer, M. *ChemPhysChem* **2005**, *6*, 2277−2285.

Figure 6. Kinetics of proteolysis of biosensor **I** by MMP-7 (42 nM). Fluorometric assays measuring initial velocity, ν, were performed at 298 K in standard buffer. Line represents best fit to Michaelis−Menten model (eq 1).

Table 2. MMP-7 Enzyme Kinetic Parameters for Different Peptide Substrates

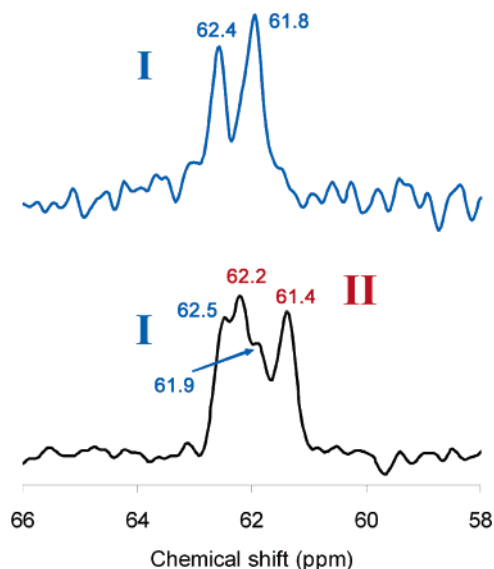| substrate	K_M (μM)	V_{max} (M s^{-1})	k_{cat}/K_M (M^{-1} s^{-1})
biosensor **I**	43	1.3×10^{-8}	7.2×10^3
N$_3$-CH$_2$CH$_2$-CONH$_2$-RKRPLALWRSRK **1**	150	4.7×10^{-8}	7.3×10^3
dinitrophenyl-RPLALWRS^a	26	−	1.9×10^5

^{a} MMP-7 activity toward this fluorogenic substrate was reported previously at 303 K.[38]

exploring this interaction by alternate spectroscopic methods. This is a useful application of Trp fluorescence quenching to monitor a biochemical reaction. For monitoring the enzymatic cleavage process at longer times ($t > 20$ min; Figure 3, a and b), the HPLC data were a more transparent indicator of reaction progress, based on defined substrate and product peaks. In the fluorometric assay, the Trp fluorescence decreased linearly for the first 20 min but showed little apparent decrease after 30 min, which was likely due to the diminishing concentrations of Trp (**3**) and free cryptophane (**II**) in solution. By monitoring initial velocities, it was possible to circumvent this problem and obtain data in good agreement with the less sensitive HPLC assay.

Future hyperpolarized ^{129}Xe MRI studies are likely to be conducted with in vivo concentrations of $10-100$ μM biosensor*hyperpolarized ^{129}Xe complex, based on considerations of biosensor delivery, as well as hyperpolarized ^{129}Xe lifetime in solution and sensitivity. Thus, the efficiency of the MMP-7 cleavage reaction for biosensor **I** was compared to that for the cognate peptide **1** over this biosensor concentration range. The cleavage of **I** was monitored both fluorometrically and by HPLC UV−vis measurements, whereas **1**, which lacked a cryptophane quencher, was monitored only by HPLC. Enzyme reaction parameters were determined from measuring the initial consumption of $10-15$% of each substrate. The k_{cat}/K_M value was calculated by nonlinear regression of the enzyme activity data at different concentrations of **I**, as shown graphically in Figure 6 and tabulated in Table 2. The data showed that **1** and **I** were similarly specific substrates for MMP-7 with virtually identical values for k_{cat}/K_M. MMP-7 showed higher affinity for biosensor **I** ($K_M = 43$ μM) than the more natural substrate **1** ($K_M = 150$ μM). One explanation for the 3.6-fold lower V_{max} for biosensor **I** could be stabilization of the enzyme−product complex by the cryptophane, but this remains to be tested in the lab.

Both substrates were comparable in affinity to the previously studied, fluorescently labeled MMP-7 consensus sequence, dinitrophenyl-RPLALWRS ($K_M = 26$ μM),[38] but showed

Figure 7. Hyperpolarized [129]Xe NMR spectra in D_2O of biosensor **I** alone (above, blue trace, 154 μM) and a mixture of intact (**I**, 77 μM, blue labels) and cleaved sensors (**II**, 95 μM, red labels).

roughly 25-fold lower specificity. Substrates **1** and **I** differed from this fluorogenic peptide with charged arginine and lysine residues at both the C- and N-termini. It appears likely that these residues were responsible for decreasing enzyme specificity and, thereby, lowering K_{cat}/K_M. The two RK units were incorporated into biosensor **I** in order to improve water solubility and to modulate the electrostatic environment near the cage, but it should be possible to remove these residues and improve substrate specificity. Through these studies, the promising observation was made that the cryptophane had a modest effect on enzyme activity when placed ~35 Å from the MMP-7 cleavage site. Thus, future biosensors can incorporate the enzyme-reactive site much closer to the cage, which will provide additional avenues for modulating the [129]Xe chemical shift. We reiterate that the incorporation of a single Trp within the biosensor provided valuable insight into the molecular structure in solution and greatly facilitated the enzymatic assays. Future biosensor designs are likely to benefit from also placing tryptophan within the peptide sequence, in some cases much closer to the cryptophane, in order to promote intramolecular quenching.

[129]Xe NMR. Hyperpolarized [129]Xe NMR experiments clearly revealed differences in the xenon environment between the intact biosensor **I** and MMP-7-cleaved product **II** (Figure 7). The concentration of each compound was determined by UV−vis absorbance measurements at 280 nm in water: ϵ_{280} = 15,000 M^{-1} cm^{-1} for the intact biosensor and ϵ_{280} = 9300 M^{-1} cm^{-1} for the cleaved biosensor. Chemical shift assignments were based on using free [129]Xe in D_2O at 186.2 ppm as the reference. Raw Fourier transforms were fitted to the double and quadruple Lorentzian line forms prior to applying 20-Hz Gaussian broadening. As shown in Figure 7, each spectrum of intact and cleaved Xe biosensors consisted of two peaks separated by 0.6 and 0.8 ppm, respectively, which were attributed to diastereomers of the peptide-cage conjugates (RL and LL) that originated from the chirality of the two components, peptide and cryptophane-A.[12,13] The two diastereomer peaks for **I** (Figure 7, top trace) were at 61.8 and 62.4 ppm with linewidths of 28 and 22 Hz, respectively. In a separate measurement (see Supporting

Information), **II** gave two peaks with very similar chemical shifts, −0.1 ppm and +0.1 ppm for the two diastereomer peaks. According to calculations by Harris et al.,[69] the difference in the diastereomer separation might be due to the difference in the electrostatic potential between intact and cleaved Xe biosensor.[15,16] The diastereomers also showed distinct Xe-binding properties evidenced from the different linewidths they exhibited individually.[15,16] Because the [129]Xe chemical shift is known to be temperature dependent (~0.28 ppm per °C)[13] and it was not possible to control the sample temperature precisely in the home-built NMR spectrometer during the data acquisition, a mixed solution of **I** and **II** was prepared to indicate the difference in [129]Xe chemical shift. As shown in Figure 7, two sets of peaks, major (frequency = 61.4, 62.2 ppm; line width = 25, 21 Hz) and minor (frequency = 61.9, 62.5 ppm; line width = 26, 21 Hz), were observed in the mixed solution. Based on the concentrations of **I** and **II** (77 and 95 μM, respectively), the major peaks were assigned to Xe encapsulated in the cleaved biosensor **II**, and the minor peaks were due to Xe in the intact biosensor **I**. The area under each set of peaks was consistent with this assignment. Furthermore, the chemical shift differences between the two major and two minor peaks were 0.8 and 0.6 ppm, respectively, which is in agreement with the difference between diastereomer peaks for the cleaved and intact Xe biosensors.

Discussion

Reasons for the difference in [129]Xe chemical shift between the two compounds have not yet been fully elucidated, but the previously described fluorescence experiments help to rule out several possible explanations. Intra- and intermolecular interactions were found to be insignificant in **I** and **II** and thus are unlikely to make substantial contributions to the Xe-binding environment. Similarly, it is unlikely that the rotational correlation time differs sufficiently between the two compounds to produce the observed difference in [129]Xe chemical shift. A substantial interaction was identified between cryptophane-A and the Trp-containing hexapeptide, but only after enzymatic cleavage, and **3** was absent from the [129]Xe NMR experiments. It appears that dissimilar electrostatic environments of the Xe-binding cages in **I** and **II**, produced by the difference in charge (+3) between the two peptides, resulted in the observed 0.5 ppm change in [129]Xe chemical shift for one pair of diastereomers, and 0.3 ppm for the other pair. The small change in [129]Xe chemical shift may be due to the large distance of the tryptophan and C-terminal positively charged residues from the cryptophane, and the limited intra- and intermolecular interactions at rt. It is postulated that the positively charged (RK) C-terminus of **I** distorted the xenon electron cloud, despite its 50-Å separation from the cryptophane. The remarkable ability of xenon to sense its remote environment presents many opportunities for the development of enzyme-specific [129]Xe magnetic resonance biosensors. Information gained from these enzymatic assays and fluorescence experiments will make it possible to design biosensors that produce much larger changes in [129]Xe chemical shift, while maintaining catalytic efficiency.

Efforts to develop [129]Xe biosensors as cancer diagnostic agents will benefit from previous applications of hyperpolarized

(69) Sears, D. N.; Jameson, C. J.; Harris, R. A. *J. Chem. Phys.* **2004**, *120*, 3277−3283.

[129]Xe for in vivo imaging. Hyperpolarized [129]Xe MRI has been performed on the bodies and brains of rats,[4,70−72] the lungs of mice,[2] dogs,[73] and humans,[1] and in animal tumors.[5] Hyperpolarized [129]Xe is typically delivered in vivo by inhalation or through direct injection of xenon-saturated perdeuterated or perfluorocarbon solutions.[70] Pines and co-workers recently demonstrated the application of xenon biosensors in heterogeneous mixtures by obtaining MR images of the biotin-labeled biosensor attached to avidin-coated agarose beads.[15] These studies represent significant advances, but the development of [129]Xe biosensors for cancer imaging applications requires additional investigations: for example, the cytotoxicity of cryptophanes, the specificity of [129]Xe biosensors for cancer cell receptors, and mechanisms for generating larger [129]Xe NMR chemical shifts and higher affinity xenon-binding cages that expand the chemical shift window for multiplexing experiments. An important proof-of-principle experiment will come from our ability to distinguish healthy cells from cancer cells by [129]Xe NMR.

Current limitations in developing [129]Xe MRI contrast agents for in vivo studies include the difficulties of synthesizing large quantities of functionalized cryptophanes and delivering laser-polarized [129]Xe to living tissue. Improved methods for synthesizing xenon biosensors are crucial to developing this technology for in vivo applications. Because the lifetime of hyperpolarized [129]Xe is relatively short in biological fluids,[3,4,74] it will be important that hyperpolarized [129]Xe can be continuously delivered to the site of the cryptophane in order to maintain signal intensity. Thus, one possible application of xenon biosensors is the [129]Xe MR spectroscopic identification of biomarkers in the lungs, where hyperpolarized xenon can be delivered through semi-continuous inhalation. New techniques for generating multiliter quantities of highly polarized [129]Xe will facilitate efforts to conduct [129]Xe MRI experiments in human patients.[75]

Conclusion

In summary, we developed an efficient synthesis for an enzyme-responsive [129]Xe biosensor consisting of a modified cryptophane-A cage and peptide substrate. The cryptophane, despite its hydrophobicity and steric bulk, did not interfere with MMP-7 activity at relevant biosensor concentrations. Enzyme cleavage produced a maximum change in [129]Xe chemical shift of 0.5 ppm for one pair of diastereomers. The average change in [129]Xe chemical shift, including both pairs of diastereomers, was 0.4 ppm. Hyperpolarized [129]Xe NMR experiments detected proteolysis from just picomoles of MMP-7, based on the catalytic efficiency of this enzyme to cleave biosensor **I**. These experiments indicated that future biosensors can place the cleavage site much closer to the Xe-binding cage in order to modulate the [129]Xe chemical shift. A strong interaction, $K_S = 9000 \pm 1000$ M^{-1}, was identified between a tryptophan-containing hexapeptide and the aromatic-rich cryptophane. Specific interactions between cryptophanes and peptides provide new avenues to modulate the [129]Xe chemical shift for biosensing applications.

Supporting Information Available: Multistep synthesis of biosensors, solid-phase synthesis, temperature dependence of Trp fluorescence for **I** and **3**, and [129]Xe NMR spectrum for biosensor **II**. This material is available free of charge via the Internet at http://pubs.acs.org.

JA0640501

(70) Venkatesh, A.; Zhao, L.; Balamore, D.; Jolesz, F.; Albert, M. *NMR Med.* **2000**, 245−252.
(71) Welsh, R. C.; Chupp, T. E.; Coulter, K. P.; Rosen, M. S.; Swanson, S. D.; Agranoff, B. W. *Nucl. Instrum. Methods Phys. Res., Sect. A* **1998**, *402*, 461−463.
(72) Nakamura, K.; Kondoh, Y.; Wakai, A.; Kershaw, J.; Wright, D.; Kanno, I. *Magn. Reson. Med.* **2005**, *53*, 528−534.
(73) Ruppert, K.; Brookeman, J. R.; Hagspiel, K. D.; Driehuys, B.; Mugler, J. P. *NMR Biomed.* **2000**, *13*, 220−228.
(74) Wolber, J.; Cherubini, A.; Leach, M. O.; Bifone, A. *Magn. Reson. Med.* **2000**, *43*, 491−496.

(75) Ruset, I. C.; Ketel, S.; Hersman, F. W. *Phys. Rev. Lett.* **2006**, *96*, 053002.